Fitoterapia 89 (2013) 20–32

Contents lists available at SciVerse ScienceDirect

Fitoterapia

journal homepage: www.elsevier.com/locate/fitote

Structure and antioxidant activity study of sulfated acetamido-polysaccharide from *Radix Hedysari*☆

Zilong Dang [a], Demei Feng [b], Xiaohua Liu [a], Tao Yang [a], Long Guo [a], Jin Liang [a], Jiandi Liang [a], Fangdi Hu [a], Fang Cui [a], Shilan Feng [a,*]

[a] School of Pharmacy, Lanzhou University, 199 Donggangxi Road, Lanzhou 730000, PR China
[b] The Second People's Hospital of Gansu Province, Hezhengxi Road 388, Lanzhou 730000, PR China

ARTICLE INFO

Article history:
Received 17 January 2013
Accepted in revised form 8 May 2013

Keywords:
Radix Hedysari
2D NMR
Structure
Polysaccharide
Atomic force microscopy
Electron microscopy

ABSTRACT

A new sulfated acetamido-heteropolysaccharide, HPS4-2A, was obtained by aqueous extraction followed by precipitation with ethanol and fractionation with DEAE column chromatography from *Radix Hedysari*. It was composed of rhamnose, arabinose, glucose, galactose and 2-acetamido-2-deoxy-D-galactose in the molar ratio of 10.09%:25.90%:25.90%:25.0%:12.30%. Elemental analysis indicated that HPS4-2A was a sulfated polysaccharide containing small amount of sulfate groups (1.87%). Partial acid hydrolysis, GC, GC–MS, 1D and 2D NMR spectroscopy analysis of the HPS4-2A revealed a predominance of glucose, galactose and 2-acetamido-2-deoxy-D-galactose linked in a highly-branched structure. The molecular weight of HPS4-2A was determined by HPSEC and HPSEC-MALLS. AFM study indicated that HPS4-2A took a highly branched conformation, which in consistent with the result studied by SEC-MALLS. Structural features of HPS4-2A were also investigated by SEM and TEM. Antioxidant assays demonstrated that HPS4-2A possessed of strong DPPH and hydroxyl radicals scavenging activities, suggesting that HPS4-2A could potentially be used as natural antioxidant.

1. Introduction

Radix Hedysari was a traditional Chinese medicine, and it is often used as a substitute for *Astragalus membranaceus (Fisch.) bge* in the folk. Distributed throughout north China, it was used to strengthen the immune system and treat diarrhea, diabetes mellitus, chronic nephritic proteinuria, inflammation and many other diseases [1,2]. The *Radix Hedysari* polysaccharides (HPS) have been reported to exhibit various pharmacological activities include enhancement of the immune system, antitumor, hypoglycemic, antioxidation and anti-aging properties [3–6]. Our research group study had shown that representative constituent of HPS2 (the second fraction of HPS) was mainly composed of dextran [7]. According to our previous study, the crude polysaccharide HPS4 (the fourth fraction of HPS) had potential radioprotective effect on acute radiation injured mice.

The physical and chemical properties of the polysaccharides (such as the molecular weight, monosaccharide composition, degree of branching, substituents and glycosidic linkages) were related with its biological activities. Elucidation of polysaccharide structure characteristic was necessary for understanding the mechanism of biological activity and expounding the structure–activity relationships [8,9].

HPS were purified into four homogeneous fractions (HPS4-1A, HPS4-1B, HPS4-1C and HPS4-2A) by DEAE-52 and Sephadex G-200 column chromatography. In this paper, the structure of main fraction (HPS4-2A) was elucidated using partial acid hydrolysis, methylation, GC, GC–MS, 1D and 2D NMR, and its conformation revealed by SEC-MALLS,

* Corresponding author. Tel./fax: +86 931 8915686.
E-mail address: fengshl@lzu.edu.cn (S. Feng).

0367-326X/$ – see front matter © 2013 The Authors. Published by Elsevier B.V. All rights reserved.
http://dx.doi.org/10.1016/j.fitote.2013.05.011

SEM, TEM and AFM. 2D NMR included COSY and TOCSY (homonuclear $^{1}H/^{1}H$ correlation spectroscopy), HSQC and HMBC (heteronulcear $^{13}C/^{1}H$ multiple-quantum correlation spectroscopy). The antioxidant activity of the HPS4-2A was evaluated in vitro by 1,1-diphenyl-2-picrylhydrazyl (DPPH) free radical and hydroxyl radical scavenging assay.

2. Experimental

2.1. Materials and general methods

2.1.1. Materials

Radix Hedysari was purchased from Wudu County (Gansu Province, China) and identified by Prof. Zhigang Ma, School of Pharmacy, Lanzhou University. The roots of *Radix Hedysari* were dried in shade and ground into powder. The standard monosaccharides, including rhamnose, arabinose, xylose, mannose, glucose, galactose, glucuronic acid and galacturonic acid were all from National Institute for the Control of Pharmaceutical and Biological Products (Beijing, China) and 2-acetamido-2-deoxy-D-galactose from Hai Hang Industry Co., Ltd (Jinan, China). DEAE-52 cellulose was purchased from Whatman Co. (Maidstone, UK), Sephadex G-200, and G-100 were purchased from Treechem (Shanghai, China). Dextran of different molecular weights (668,000, 410,000, 273,000, 148,000, 48,600, 23,800, 11,600, and 5200 Da) was purchased from PSS (USA). All chemicals used were of analytical grade unless otherwise specified.

2.1.2. General methods

Total carbohydrate content was determined by phenol-sulfuric acid method [10], with glucose and galactose as the standards at 490 nm. Protein content was assayed by Bradford method with bovine serum albumin as reference protein [11]. Uronic acid content was determined according to GC method [12], and m-hydroxydiphenyl method [13] by measuring the absorbance at 525 nm and using galacturonic acid and glucuronic acid as standards. GC analysis used a fused-silica capillary column OV-101 (60 m × 0.25 mm i.d., × 0.25 μm film thickness), and was carried out using a Shimadzu GC-2010 (Shimadzu, Japan) with flame ionization detector.

2.2. Isolation and purification of polysaccharide

The extraction process was conducted according to the earlier report [14]. Briefly, the ground dry roots of *Radix Hedysari* (4000 *g*) were extracted 3 times with tap water (40,000 ml) at 100 °C for 3 h each time. The combined aqueous extracts filtered through a cotton cloth bag and centrifuged (3000 *g* for 15 min) and then concentrated in a rotary evaporator at 60 °C. Then the aqueous solution was precipitated by 95% ethanol at a final concentration of 70% (V/V). The sediment was dissolved in water, and precipitated by 95% ethanol at a final concentration of 40% (V/V), the supernatant concentrated to a proper volume under reduced pressure and lyophilized to get the crude polysaccharide. Then, the crude polysaccharide from *Radix Hedysari*, named HPS4 was obtained after deproteinized according to Sevage method [15] and decolored by H_2O_2. HPS4 was redissolved in distilled water and precipitated by 95% ethanol (to give 40%, 70%, V/V final ethanol concentrations) to achieve two crude polysaccharides accordingly, named as HPS4-1 and HPS4-2. HPS4-2 was redissolved in distilled water and applied to a DEAE-52 column (2.7 cm × 70 cm). The column was eluted stepwise with distilled water, 0.1–1.0 M NaCl aqueous solution and fractions collected at a flow rate of 0.5 ml/min (each test tube hold 12 min) and monitored by the phenol-sulfuric acid method. Then the major fraction, named HPS4-2A (eluted by 1.0 M NaCl) was concentrated, dialyzed and lyophilized according to the elution curve. The following studies are aimed at HPS4-2A.

2.3. Elemental analysis

Elemental analysis was carried out by Elementar Vario EL instrument (Elementar, Germany) to analyze weight percentages of carbon (C), hydrogen (H), oxygen (O), sulfur (S) and nitrogen (N). Sulfated group content ($-SO_2O-Na^+$, sodium salt) was analyzed using the factor of 3.22 to convert measured weight percentage of sulfur to sulfate.

2.4. Molecular weight and homogeneity determination

2.4.1. High performance size exclusion chromatography (HPSEC)

The molecular weight and homogeneity of HPS4-2A was determined using HPSEC method, which was conducted on a Waters HPLC, including a pump (Waters 600), a RI detector (Waters 2414) and a photodiode array detector (Waters 2998). HPSEC was performed on successively linked of two columns (Ultrahydrogel™ 1000 and Ultrahydrogel™ 500 columns, 300 × 7.8 mm, waters, Massachusetts, USA) and eluted with 0.9% (W/V, 0.154 M) NaCl containing 0.02% (W/V) NaN_3 (1.0 ml/min). The temperature of columns and RI detector was maintained at 35 °C.

Dextran standards were used to establish a standard curve (retention time was horizontal axis and logarithm of molecular weight of dextrans was vertical axis). The obtained data were analyzed by Empower (Version 2.0,Waters) software.

2.4.2. HPSEC-MALLS

The molecular weight and homogeneity of HPS4-2A were also can be determined by HPSEC-MALLS method. The HPSEC-MALLS system consisted of a separation module (Waters 600), a photodiode array detector (Waters 2998) set at 280 nm, a multi-angle laser light scattering detector (Wyatt DAWN-EOS) with a laser at 690 nm, along with a refractive index monitor (Waters 2414). HPS4-2A was dissolved with mobile phase (5 mg/ml) and filtered (0.45 μm) before injection (50 μl). Then eluted with 0.9% (W/V, 0.154 M) NaCl containing 0.02% (W/V) NaN_3 (1.0 ml/min) from two columns as mentioned in Section 2.4.1. Data for molecular weight determination were analyzed using ASTRA software (Version 4.73.04, Wyatt Technology Corp.) using a dn/dc of 0.138 ml/g.

2.5. Compositional analysis

The compositional analysis of HPS4-2A was performed by the alditol acetate method [16], with minor modifications. Briefly, HPS4-2A was hydrolyzed by 2 M trifluoroacetic acid at 121 °C for 3.5 h followed by reduction in distilled water with $NaBD_4$ 1.5 h at room temperature, and subsequent acetylation

by acetic anhydride with pyridine as the catalyst at 100 °C for 1 h. The standards, including rhamnose, arabinose, xylose, mannose, glucose, galactose, 2-acetamido-2-deoxy-D-galactose, treated in parallel with sample. The alditol acetate derivatives produced were separated by GC on an DB-5MS fused silica capillary column (50 m × 0.25 mm i.d., 0.25 μm film thickness) with the GC oven programmed from 150 °C to 170 °C at a rate of 5 °C/min, and then to 225 °C at a rate of 8 °C/min, held for 1 min and then to 250 °C at a rate of 5 °C/min, hold for 5 min and detected by MS using an Varian 320-MS (320-MS is a triple quadropole mass spectrometer, Varian, USA). Identifications were based on peak retention time and by comparison of electron impact mass spectra with standard spectra, and further contrast to standard samples. Quantification of each monosaccharide was carried out by integration of the chromatographic peak area.

2.6. Partial hydrolysis analysis

HPS4-2A (50 mg) was hydrolyzed with 4 ml 0.1 M TFA at 100 °C for 1 h. After cooling, TFA was evaporated under reduced pressure. The hydrolysate was dissolved and dialyzed against distilled water (M_w cut-off 3500 Da) to obtain two fractions, inside dialysis bag fraction (HPS4-2AI) and outside dialysis bag fraction (HPS4-2AL). HPS4-2AI and HPS4-2AL were collected. Then HPS4-2AI was applied to Sephadex G-100 column (2.6 cm × 70 cm), and the major peak fractions were collected, named HPS4-2AH. HPS4-2AH and HPS4-2AL were collected for monosaccharide composition analysis by GC–MS as described in Section 2.5.

2.7. Methylation analysis

HPS4-2A (5 mg) was methylated using CH_3I and NaOH in DMSO [17]. The methylated polysaccharides were acetylated to partially methylated alditol acetates as described by [18]. The derivatives produced were analyzed by GC–MS as described in Section 2.5. Quantification of each methylated monosaccharide was determined by integration of the chromatographic peak area.

2.8. Spectrum analysis

2.8.1. IR spectrum

HPS4-2A were mixed with KBr pellets for FT-IR measurement and recorded on a Nicolet Nexus 670 spectrometer (Nicolet, USA) in the frequency range of 4000–400 cm^{-1}.

2.8.2. NMR spectrum

HPS4-2A (30 mg) was exchanged with deuterium by freeze-drying with D_2O three times. Then the sample was dissolved in 0.5 ml D_2O and ^1H and ^{13}C spectra were recorded on a Bruker NMR spectrometer (600 Hz INOVA 600NB) at 25 °C.

2.9. Ultrastructure analysis

2.9.1. Scanning electron microscope (SEM)

The powder of the HPS4-2A was directly pasted on a carbon conductive tape, and sputtered with gold (Balzers/Union FL-9496) for 1 min. The sample was observed in a JEOL JSM-6380LV scanning electron microscopy (JEOL, Tokyo, Japan), which operated at 5 kV. A working distance of 8 mm and slow scan mode were used for imaging.

2.9.2. Transmission electron microscope (TEM)

A drop of aqueous solution of HPS4-2A was first placed on a carbon-coated TEM copper grid (Quantifoil, Germany) and allowed to air-dry. The sample was then negatively stained with phosphotungstic acid (Merck, Germany): a drop phosphotungstic acid aqueous solution (1%, W/W) was dripped to the carbon-coated TEM grids. The grid was then air-dried, and put them into the electron microscope. The samples were viewed at 80 kV, using a JEOL JEM-1230 TEM (JEOL, Tokyo, Japan). All the micrographs were collected using Gatan 1.35 K × 1.04 K × 12 bit ES500W CCD camera at different magnifications from different parts of the specimens.

2.9.3. Atomic force microscope (AFM)

The sample was prepared by spreading of a dilute (1 μg/ml) polymer solution onto a freshly cleaved silicon wafer surface and successively air-drying under ambient temperature [19]. The atomic force microscopy (MultiMode 8, Bruker, Germany) was operated in the tapping-mode [20].

2.10. Assay for antioxidant activities of the HPS4-2A

2.10.1. Effect of scavenging 1,1-diphenyl-2-picryl-hydrazyl (DPPH) radicals

The DPPH free radicals' scavenging activity of HPS4-2A was analyzed by the method of literature [21–23], with some modifications. The 0.01 mmol/l solution of DPPH in 50% ethanol was prepared daily before using. One milliliter of sample solution (solvent was 50% ethanol) with different addition quantity (0.5, 1, 2, 4, 8 mg) was mixed thoroughly with 2 ml of freshly prepared DPPH and 2 ml of 50% ethanol, and then left to stand for 30 min at room temperature in the dark and the absorbance was then recorded at 517 nm against a blank. Ascorbic acid was used as reference compound. The scavenging activity to the DPPH radical was calculated using the following equation:

$$\text{Scavenging ability}\,(\%) = [1-(A_s-A_e)/A_b] \times 100\%.$$

Where A_b was the absorbance of mixed solution that consisted of 2 ml DPPH solution and 3 ml of 50% ethanol; A_s was the absorbance of mixed solution that consisted of 1 ml sample, 2 ml DPPH solution, 2 ml of 50% ethanol; and A_e was the absorbance of mixed solution that consisted of 1 ml sample and 4 ml of 50% ethanol.

2.10.2. Measurement of hydroxyl radical scavenging activity

The scavenging activity of hydroxyl radicals was investigated based on the method described by Zhang et al. [24] and with a minor modification. One milliliter test sample (0.5, 1, 2, 4, 8 mg/ml) was mixed with a solution containing 1 ml phenanthroline (5 mM), 0.4 ml phosphate buffer (50 mM, pH 7.4), 0.25 ml deionized water, 0.5 ml $FeSO_4$ (7.5 mM) and 0.1 ml H_2O_2 (1%). Then the mixture was incubated at

37 °C for 60 min. The ability to scavenge hydroxyl radicals was calculated with following equation:

$$\text{Scavenging effect}(\%) = (A_1 - A_2)/(A_3 - A_2) \times 100\%.$$

Where A_1 was the absorbance of sample measured at 510 nm using UV-1700 spectrophotometer (Shimadzu, Kyoto, Japan), A_2 was the absorbance when sample was replaced by deionized water, and A_3 was the absorbance when H_2O_2 and sample were replaced by distilled water.

3. Results and discussion

3.1. Physicochemical property of HPS4-2A

The total sugar content of HPS4-2A was 98.98%. The protein content of HPS4-2A was very low, only 0.26%. The negative result of m-hydroxydiphenyl reaction and GC method suggested that uronic acid was absent. Elemental analysis revealed that the elemental composition of HPS4-2A was C, H, O, N, S, and its content was 34.51% (mass %), 6.29%, 55.36%, 3.26% and 0.58%, respectively. The molar ratio of C/H/O was around 1:2:1, which was in line with molar ratio of three chemical elements in carbohydrate. The total content of sulfate ester ($-SO_2O-$) was 1.87%, which means approximately one sulfate ester was present per 27–32 sugar units on average.

3.2. Molecular weight and homogeneity determination

3.2.1. HPSEC

HPS4-2A showed a single symmetrical peak in HPSEC profile (mobile phase was deionized water or 0.154 M NaCl), indicating it was a homogeneous polysaccharide. HPSEC result showed its molecular weight was more than 388.0 kDa (mobile phase was 0.154 M NaCl).

3.2.2. HPSEC-MALLS

The HPS4-2A exhibits a single peak with good symmetry detected by differential refraction detector. This suggests it was a homogeneous polysaccharide in the sodium chloride aqueous solution. The RMS (root mean square) radius, weight average molecular weight (M_w), and polydispersity index (M_w/M_n) were measured to be 30.5 nm, 272.0 kDa, and 1.633, respectively. The conformation plot present to be U shapes, which indicated it was a branched molecule and in consistent with the result showed by Molar mass-versus-elution volume and RMS radius-versus-elution volume plots of HPS4-2A (the figure can be seen in Fig. A.1 of Appendix A). The plots showed that HPS4-2A had abnormal SEC elution behavior: after the normal decrease of the molar mass or RMS radius with increasing elution volume, both plots curved up.

The abnormal SEC elution behavior was caused by the "anchoring effect" [25] of branch structure of HPS4-2A. The so-called "anchoring effect" is, a branch of the branched polymer stuck in the gel pores of the gel column, which leads to extending retention time of the whole branched molecule in the gel column. Therefore, the region of high elution volumes was a mixture of small molecules and large branched molecules.

The explanations of the discrepancy of HPS4-2A's molecular weight measured by HPSEC-MALLS and HPSEC listed as follows: the HPSEC method used unbranched dextrans as standards and their monosaccharide composition containing only glucose, while HPS4-2A was a heteropolysaccharide composed of five different monosaccharides, and had more branches (this conclusion in the methylation, and the results of partial acid hydrolysis and NMR have also been confirmed) and larger molecular radius, which make a big difference between the two structure. Although the results are different and strongly depended on the methods used for analysis, the authors believe that the result of HPSEC-MALLS is much more reliable according to the above explanation.

3.3. Compositional analysis

The monosaccharide composition of HPS4-2A was analyzed by GC–MS and compared with the monosaccharide standards. The result showed that HPS4-2A was mainly composed of rhamnose, arabinose, glucose, galactose and 2-acetamido-2-deoxy-D-galactose in the molar ratio of 10.09%:25.90%:25.90%:25.0%: 12.30%.

3.4. Partial acid hydrolysis analysis

The high molecular weight fraction, HPS4-2AH, yields 44.0% of the HPS4-2A, composed of rhamnose (6%), arabinose (0.4%), glucose (40.8%), galactose (33.6%) and 2-acetamido-2-deoxy-D-galactose (19.2%). The lower molecular weight fraction, HPS4-2AL, the sugar compositions showed that arabinose (35.8%) and glucose (41.9%) were the main constituents and with a relatively small amount of rhamnose (15.1%) and galactose (6.7%). For HPS4-2AH, the amount of arabinose and rhamnose decreased considerably compared with HPS4-2A, whereas the amount of glucose, 2-acetamido-2-deoxy-D-galactose and galactose increased. According to above data, the main backbone of HPS4-2A was composed of glucose, galactose and 2-acetamido-2-deoxy-D-Gal, and substituted by the side chains of mainly arabinosyl and glucosyl residues.

3.5. Methylation analysis

The total ion current peaks from the partially methylated alditol acetates (PMAA) were identified by their retention time, characteristic ion fragments in MS spectra libraries and contrast to referenced literatures [26]. The molar ratio of methylated monosaccharide residues was calculated based on the integral area of peaks. The majority of the terminal units were T-L-Araf (18.25%), with relatively small amount of T-Glcp (9.76%). The branched sugar residues →4,6) Glcp (1→, →3,6) Galp (1→, →4,6) Galp (1→, →2,4) Rhap (1→ and →3,4) 2-NAc-Galp (1→ with the molar ratio of 12.30%, 5.90%, 5.68%, 5.12% and 0.86%, respectively. The unsubstituted sugar residues were shown to be →2) Rhap (1→, →5) Araf (1→, →6) Galp (1→, →4) Glcp (1→ and →6) Glcp (1→, in percentage of 12.06%, 11.46%, 6.42%, 6.15% and 5.86%, respectively. Although low values for the proportion of partially methylated amino sugars were not uncommon, smaller amounts of partially methylated 2-acetamido-2-deoxy-D-galactose (0.86%) were obtained. It was unclear why a low yield of the acetamino sugar was

obtained in the methylation analysis. In addition, there was trace amount of →2,3,4) Galp (1→ (0.18%) and T-Rhap (trace) existed, this may be caused by side reactions in the methylation process. According to the data of the methylation, and then combined with the results of the partial acid hydrolysis, we can tentatively draw the following conclusions: HPS4-2A was mainly composed of →4,6) Glcp (1→, →4,6) Galp (1→, →3,6) Galp (1→, →3,4) 2-NAc-Galp (1→ as the backbone with some →5) Araf (1→, →2) Rhap (1→, →4) Glcp (1→ and →6) Glcp (1→, which maybe exist in the side chains.

3.6. Spectrum analysis

3.6.1. IR spectrum

The evidence of sulfate ester was confirmed by the appearance of the peaks at 817.8 (very weak) and 1240.71 cm^{-1} (Figure not given), which was originated from the bending vibration of C – O – S of sulfate in axial position and stretching vibration of S – O, respectively. The absorption in the range of 1200–1000 cm^{-1} that appeared in IR spectrum indicated that the monosaccharide in HPS4-2A had a pyranose ring. The strong absorption peak at 1615.08 cm^{-1} and the weak one at 1414.40 cm^{-1} also demonstrated the characteristic IR absorption of polysaccharide. The strong signal at 3407.27 cm^{-1} was from stretching vibration of N – H and O – H. Unfortunately, the signal of carbonyl stretching, $\nu_{C=O}$ (amide I), and the NH bending, δ_{NH} (amide II), was not observed.

3.6.2. NMR spectrum

The HPS4-2A was further analyzed by 1D and 2D NMR spectroscopy. The ^{13}C and ^{1}H assignments for the HPS4-2A were reported in Table 1 and were assigned on the basis of 2D COSY, TOCSY, HSQC, and HMBC experiments, along with reference to the published data for similar molecules. The ^{1}H NMR spectrum (Figure not given) showed more than six peaks in the anomeric region, the dominant peaks were centered on δ 5.00 and 4.40 ppm. These overlapping peaks can be clearly observed in the anomeric area of the HSQC (Fig. 1a). For example, from δ 4.85 ppm to δ 5.4 ppm, eight cross peaks were observed, with the corresponding ^{13}C chemical shifts identified as δ 108.0, 107.5, 102.0, 101.4, 101.0, 100.0, 99.5 and 97.5 ppm respectively. In the region of δ 4.3 ppm to δ 4.8 ppm, there were four major cross peaks with their ^{13}C chemical shifts identified at δ 104.6, 104.0, 104.0 and 102.8 ppm, respectively. The signal at δ 19.8 ppm belongs to the methyl group of rhamnose in ^{13}C NMR spectrum; the resonances at δ 1.10 ppm and 1.20 ppm in the HSQC spectrum showed that the rhamnose was in two different chemical environments. The ^{13}C signal at δ 22.9, 179.3 ppm and an upfield proton chemical shift at δ 2.04 ppm and a downfield proton chemical shift at δ 8.20 ppm indicated that a NAc group was present. HSQC spectrum showed twelve cross peaks in the anomeric region, which indicated that around twelve spin systems were present in HPS4-2A. The anomeric chemical shifts of sugar residues were designated as follows: δ 5.06, 107.5 for residue A, δ 5.24, 108.0 for residue B, δ 4.76, 104.0 for residue C … and δ 4.42, 102.8 for residue L (Table 1).

3.6.2.1. Assignment of residue D (→2,4) α-L-Rhap (1→). The H-1 signal of residue D at δ 5.38 ppm indicated that it was an α-linked residue. Residue D was pyran rhamnose due to the signal for an exocyclic-CH_3 group (H-6, δ 1.20 ppm). According to the COSY spectrum, the chemical shift of the H-5 (δ 3.64 ppm) could be assigned from its correlation with H-6. Base on the connectives between H-1 and H-2, H-2 and H-3, H-3 and H-4, H-2 to H-4 were assigned and their cross peaks were marked in Figs. 2 and 3a. The ^{13}C chemical shifts

Table 1
^{13}C and ^{1}H NMR assignments for HPS4-2A.

Sugar residues and sugar type	C-1/H-1	C-2/H-2	C-3/H-3	C-4/H-4	C-5/H-5	C-6/H-6
A →5) α-L-Araf (1→	107.5	82.2	76.0	81.5	68.2	–
	5.06	4.15	4.00	4.20	3.79/3.91	
B α-L-Araf (1→	108.0	81.3	76.0	85.0	62.4	–
	5.24	4.18	3.96	4.10	3.71/3.66	
C →3,6) β-D-Galp (1→	104.0	72.4	82.6	69.5	73.9	70.8
	4.76	3.77	3.86	4.20	3.79	3.87/3.78
D →2,4) α-L-Rhap (1→	100.0	77.3	73.2	82.0	71.5	19.8
	5.38	4.18	3.97	3.81	3.64	1.20
E →2) α-L-Rhap (1→	101.0	76.2	71.8	74.2	70.2	19.8
	5.24	4.08	3.81	3.48	3.70	1.10
F α-D-Glcp (1→	99.5	72.4	73.4	74.0	73.9	63.8
	4.87	3.76	3.94	3.66	3.54	3.90
G →4) α-D-Glcp (1→	102.0	73.9	76.0	79.6	71.5	63.0
	5.20	3.44	3.95	3.77	3.68	3.56/3.42
H →6) α-D-Glcp (1→	97.5	73.3	75.3	71.8	70.6	69.2
	4.98	3.82	3.62	3.74	3.93	4.19/3.88
I →6) β-D-Galp (1→	104.6	72.0	73.0	71.0	74.6	69.6
	4.57	3.44	3.66	3.91	3.88	3.98
J →4,6) β-D-Galp (1→	104.0	72.3	75.0	78.5	75.3	71.3
	4.38	3.55	3.66	4.14	3.88	3.72
K →4,6) α-D-Glcp (1→	101.4	74.2	75.7	76.2	73.2	76.1
	4.96	3.60	3.65	3.42	3.68	4.01
L →3,4)2-NAc-β-D-Galp (1→	102.8	52.4	82.0	74.3	74.0	62.0
	4.42	4.04	4.00	4.20	3.76	3.80

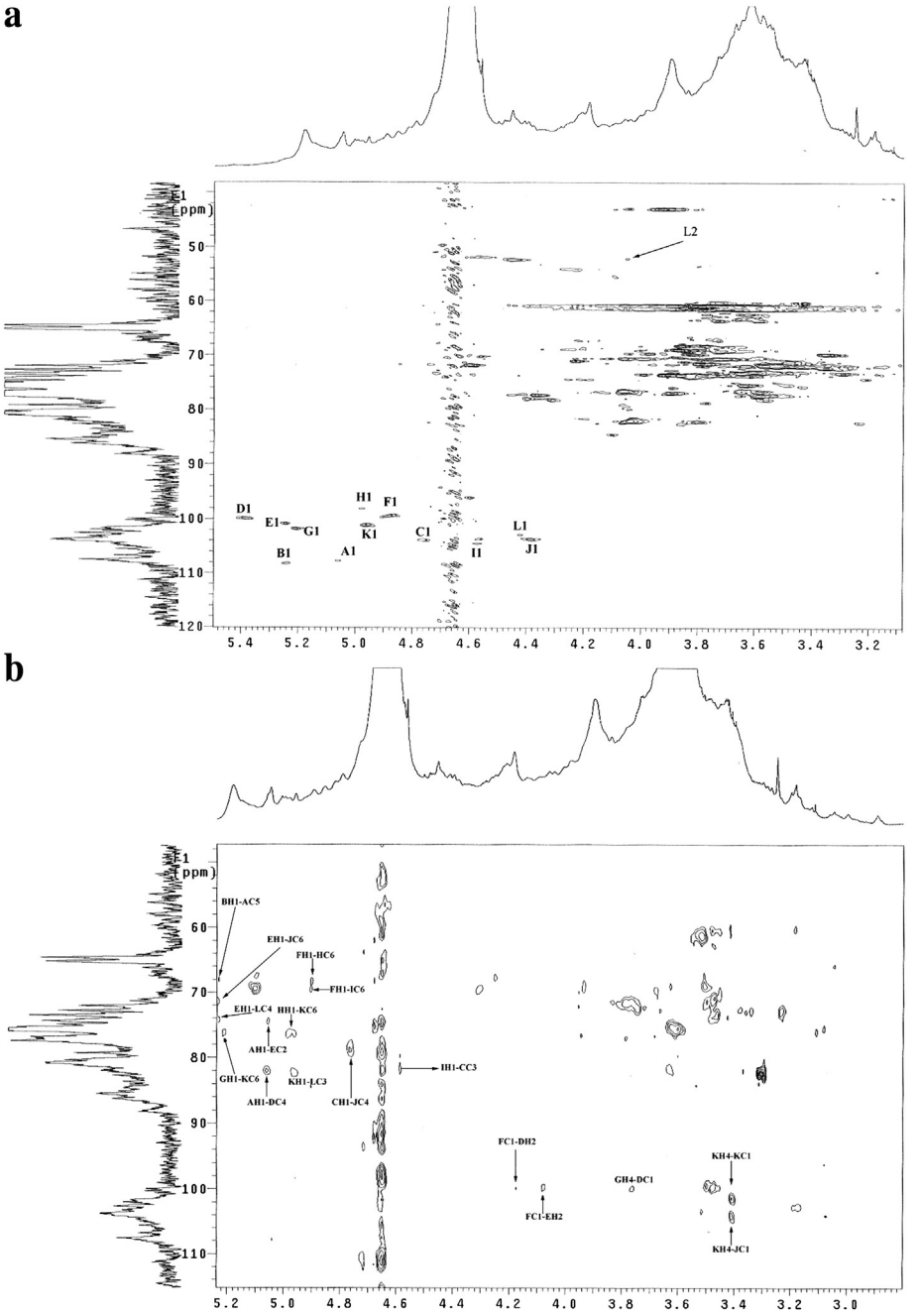

Fig. 1. 2D HSQC (a) and HMBC (b) nuclear magnetic resonance spectrum of HPS4-2A in D_2O at 25 °C.

were assigned according to the HSQC spectrum. The ^{13}C chemical and ^{1}H shifts of the →2,4) α-L-Rhap (1→ residue corresponding to the literature values [9,27,28].

3.6.2.2. Assignment of residue E (→2) α-L-Rhap (1→). The anomeric cross peak signals of residue E (δ 5.24 ppm) were shown in the HSQC spectrum. The connection between H-1 and H-2 could obtain from COSY spectrum (Fig. 2), but it was difficult to recognize the connectives between H-3 and H-4 due to overlapping in the region 3.40–3.80 ppm. In the TOCSY spectrum (Figure not given), we could observe three cross peaks (δ 3.81 ppm, δ 3.70 ppm, δ 3.48 ppm) were correlated to H-1 (δ 5.24 ppm) of residue E. Hence residue E was tentatively assigned to be → 2) α-L-Rhap (1 → by comparison with literature values [9,26]. Then the correlation between H-6 (δ 1.10 ppm) and H-5 (δ 3.70 ppm) was observed when we came back to the COSY spectrum. After the protons from H-1 to H-6 had been identified, the chemical shifts of ^{13}C were assigned (Table 1) from the HSQC spectrum and they were matched well with literature [9,26].

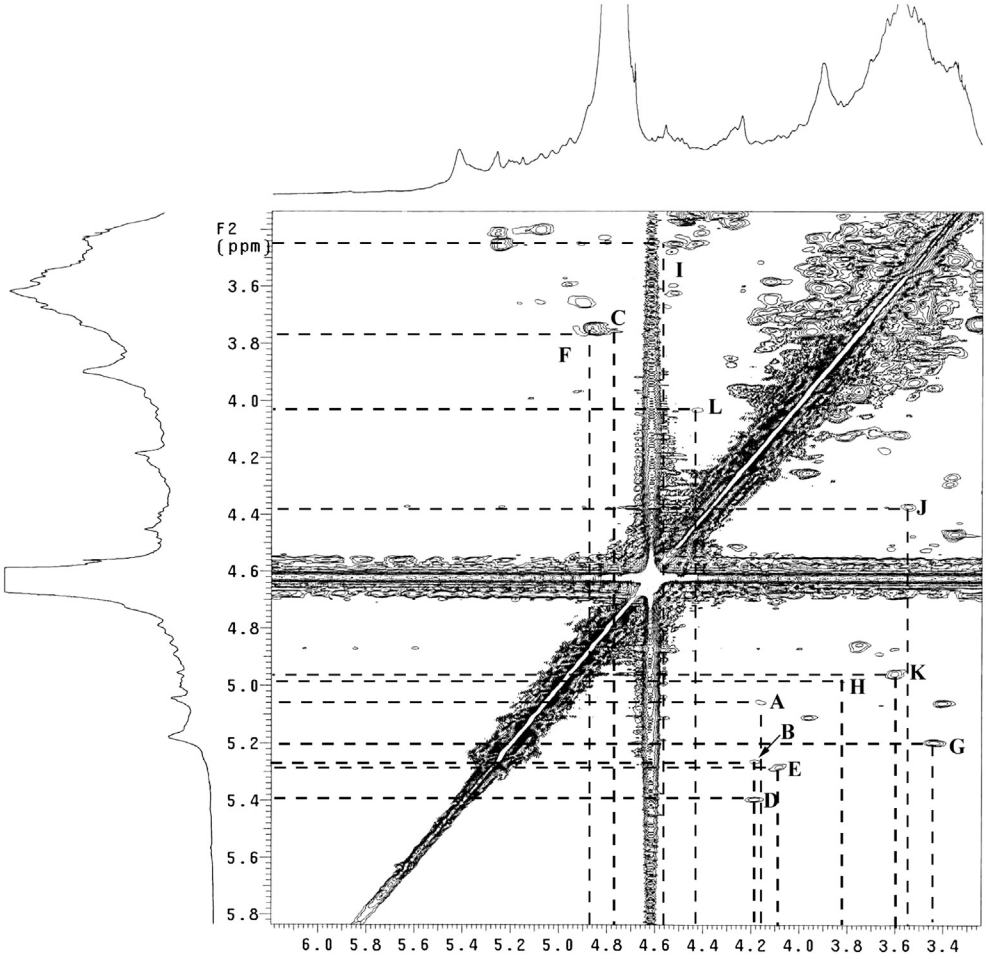

Fig. 2. COSY spectrum of HPS4-2A, the dotted lines is the connective between H-1 and H-2 of all residues.

3.6.2.3. Assignment of residue F (α-D-Glcp(1→)). Anomeric proton signal of residue F at δ 4.87 ppm indicated that it was an α-linked residue, which was confirmed by C-1 signal at δ 99.5 ppm according to HSQC spectrum. In Figs. 2 and 3b, we could observe stepwise connectivities from the H-1 signal at δ 4.87 to H-2 at δ 3.76, H-3 at δ 3.94, H-4 at δ 3.66, H-5 at δ 3.54, and H-6 at δ 3.90. From TOCSY spectrum, we also could found the relation between H-1 (δ 4.87 ppm), and H-2 (δ 3.76 ppm), and H-3 (δ 3.94 ppm). The ^{13}C chemical shifts (Table 1) of residue F were obtained from HSQC spectrum, and they were all in consistent with the previous information [7,29–31]. From the results of methylation analysis and NMR experiments, it could be concluded that residue F was terminal α-D-glucose.

3.6.2.4. Assignment of residue G (→4) α-D-Glcp (1→). Residue G had a downfield anomeric proton signal at δ 5.20 ppm indicated that it was an α-linked residue. The chemical shifts of H-2, H-3, H-4, H-5, H-6 and H-6′ were obtained from COSY spectrum (Figs. 2 and 3c) according to the stepwise connectives from H-1. After the protons had been identified, the chemical shifts of their corresponding carbons (Table 1) were determined from the HSQC spectrum. The chemical shifts assigned above, all in consistent with the previous literature of →4) α-D-Glcp (1→ [7,30–33].

3.6.2.5. Assignment of residue K (→4, 6) α-D-Glcp (1→). We could know from the results of the methylation, the content of →4, 6) α-D-Glcp (1→ was 12.30% in HPS4-2A. In the HSQC spectrum, residue K had a strong cross peak between ^{1}H-1 (δ 4.96 ppm) and ^{13}C-1 (δ 101.4 ppm), indicating that it was α-linked. It was determined as →4,6) α-D-Glcp (1→. The chemical shifts from H-1 to H-4 were assigned from 2D COSY (Figs. 2 and 3d). Although the cross peak of H-5, 6 was difficult to assign due to overlapping in the region δ 3.50–4.10 ppm, when referring to the chemical shifts of →4,6) α-D-Glcp (1→ in the literature [30,32], H-5 and H-6 can be assigned as δ 3.68 and δ 4.01 ppm, respectively. The chemical shifts of H-6 (δ 4.01 ppm) obtained by TOCSY spectrum, further conformed data obtained from literature. Their ^{13}C chemical shifts corresponding to ^{1}H were assigned from the HSQC spectrum. All the chemical shifts assigned were matched well with literature [30,32].

3.6.2.6. Assignment of residue L (→3,4) 2-NAc-β-D-Galp (1→). In the HSQC spectrum, we could observe residue L had a cross

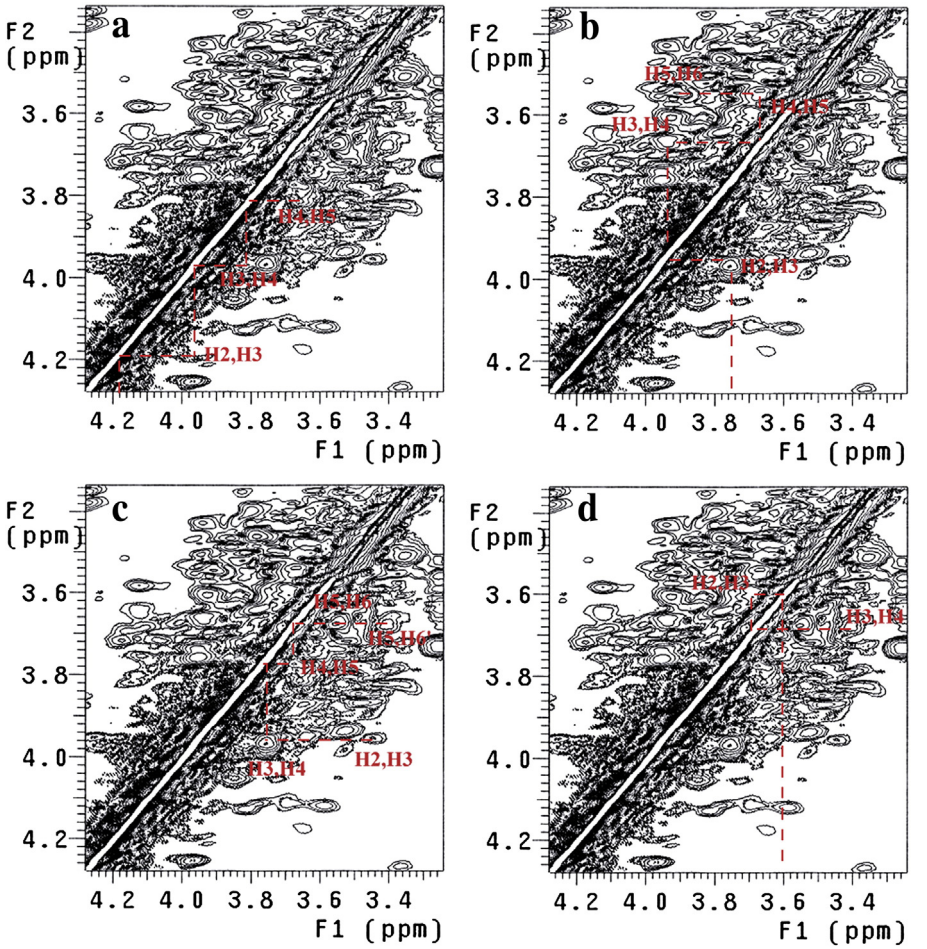

Fig. 3. Enlargement of COSY spectrum of HPS4-2A, the dotted lines are the correlations of protons of→2, 4) α-L-Rhap (1→ (a), α-D-Glcp (1→(b), →4) α-D-Glcp (1 → (c) and →4,6) α-D-Glcp (1→ (d), respectively.

peak between ^{1}H-1 (δ 4.42 ppm) and ^{13}C-1 (δ 102.8 ppm), indicating that it was a β-linked residue. The assignment of H-2 (δ 4.04 ppm) was conducted by its correlation with H-1 signal at δ 4.42 ppm in the COSY spectrum (Fig. 2). The assignment of H-3 (δ 4.00 ppm), H-4 (δ 4.20 ppm) and H-5 (δ 3.76 ppm) according to data from TOCSY spectrum and the literature values [34–36]. The allocation of H-6 resonance of residue L was supported by comparison with previous reports [34–36]. The ^{13}C chemical shifts of residue L were obtained from HSQC, and they were all in consistent with the previous information [34–36]. The ^{13}C signal at δ 22.9, 179.3 ppm and an upfield proton chemical shift at δ 2.04 ppm and a downfield proton chemical shift at δ 8.20 ppm indicated that an NAc group was present. The correlation (Fig. 1a) of the resonance between H-2 (δ 4.04 ppm) and C-2 (δ 52.4 ppm) indicated residue L was a 2-acetamido-2-deoxyglycose. Based on above results, we confirmed that residue L was →3, 4) 2-NAc-β-D-Galp (1→.

3.6.2.7. Assignment of remaining residues. In the HSQC spectrum, residues A, B, C, H, I and J had anomeric proton chemical shifts at δ 5.06, 5.24, 4.76, 4.98, 4.57 and 4.38 ppm, respectively. Because of weak and overlapping signals in the spectrum, they could only be partially assigned. The connective between H-1 and H-2 of the residues could obtain from COSY spectrum (Fig. 2) and the anomeric carbon chemical shifts could obtain from HSQC spectrum. Based on the above information, as well as the previous literature values [9,27,31,37–40], the residues A, B, C, H, I and J were assigned to be →5) α-L-Araf (1→, α-L-Araf (1→, →3,6) β-D-Galp (1→, →6) α-D-Glcp (1→, →6) β-D-Galp (1→ and →4,6) β-D-Galp (1→, respectively, and their chemical shifts were all summarized in Table 1. Proton signals of H-2 (δ 4.15 ppm) of residue A and H-2 (δ 3.44 ppm), H-3 (δ 3.66 ppm) and H-5 (δ 3.88 ppm) of residue I were further confirmed by TOCSY spectrum.

It was worth noting that near residue I had an anomeric proton and carbon chemical shift at δ 4.56 ppm, δ 103.8 ppm respectively in HSQC spectrum, suggesting that there was doublets coexist with residue I. This indicated that the residue I might have two chemical environment. Indeed, lowfield chemical shift values for C-6 (69.6) and H-6 (3.98 ppm) of residue I [41] suggest glycosylation or an electron withdrawing group exists in this position.

Table 2
The significant $^{3}J_{H,C}$ connectivities observed in an HMBC spectrum for the anomeric protons/carbons of the sugar residues of HPS4-2A.

Sugar residues and sugar linkages	H-1/C-1	Observed connectivities		
	δ H/δ C	δ H/δ C	Residue	Atom
A →5) α-L-Araf (1→	5.06	82.0	D	C-4
		74.2	E	C-2
	107.5			
B α-L-Araf (1→	5.24	68.2	A	C-5
	108.0			
C →3,6) β-D-Galp (1→	4.76	78.5	J	C-4
	104.0			
D →2,4) α-L-Rhap (1→	5.38			
	100.0	3.77	G	H-4
E →2) α-L-Rhap (1→	5.24	71.3	J	C-6
		74.3	L	C-4
	101.0			
F α-D-Glcp (1→	4.87	69.2	H	C-6
		69.6	I	C-6
	99.5	4.18	D	H-2
		4.08	E	H-2
G →4) α-D-Glcp (1→	5.20	76.1	K	C-6
	102.0			
H →6) α-D-Glcp (1→	4.98	76.1	K	C-6
	97.5			
I →6) β-D-Galp (1→	4.57	82.6	C	C-3
	104.6			
J →4,6) β-D-Galp (1→	4.38			
	104.0	3.42	K	H-4
K →4,6) α-D-Glcp (1→	4.96	82.0	L	C-3
	101.4	3.42	K	H-4

3.6.3. Linkage sites and sequence among residues

A long-range HMBC experiment performed on the HPS4-2A enable us to identify linkage patterns between sugar residues, as shown in Fig. 1b, and summarized in Table 2. In this experiment, the correlations of the resonances between protons and carbon atoms help us define what kind of glycoside linkage that connects two sugar residues. The cross peaks of anomeric protons and carbons of each sugar residue of HPS4-2A were determined and inter-residual connectivity was observed in HMBC spectrum. For example, cross peaks were found between C-1 (δ 101.4 ppm) of residue K and H-4 (δ 3.42 ppm) of residue K (K C-1, K H-4), H-1 (δ 4.96 ppm) of residue K and C-3 (δ 82.0 ppm) of residue L (K H-1, LC-3). Cross peaks between C-1 (δ 99.5 ppm) of residue F and H-2 (δ 4.18 ppm, 4.08 ppm) of residue D and E (F C-1, D H-2 and F C-1, E H-2) were observed in the same way, indicating that some of the terminal glucopyranosyl residues were linked with →2) α-L-Rhap (1→ by 1,2-O-glycosidic bonds. With the same method, the cross peaks of other residues were found and summarized in Table 2.

Unfortunately, the position of sulfate group in HPS4-2A can't be determined by NMR spectra. But according to the data obtained, we speculate that the most likely connection position of sulfate group at O-6 of residue I, and we will further study the location of the sulfate group of HPS4-2A in the subsequent research.

As a result of all the structural information described, a possible molecular structure of HPS4-2A was proposed as in Fig. 4.

3.7. Ultrastructure analysis

To provide direct evidence of the chain conformation of the polysaccharides, SEM, TEM and AFM were used to observe their morphology.

3.7.1. Scanning electron microscope

Morphological of HPS4-2A was observed using SEM after lyophilized. The SEM images showed thin lamellar structure that is probably due to shrinkage occurring during the water evaporation of polysaccharide solution while drying. This phenomenon is more evident for the freeze-dried samples [42]. The high magnification image of HPS4-2A showed smooth surface appearance. SEM images of HPS4-2A can be seen in Fig. A.2(a and b) of Appendix A.

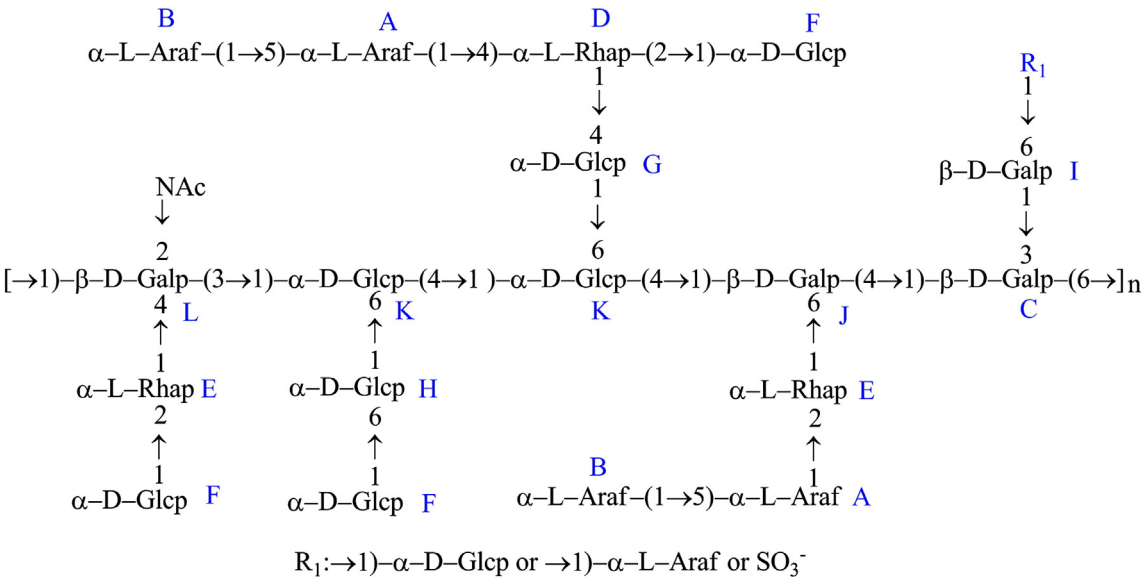

Fig. 4. Proposed structure of HPS4-2A.

3.7.2. Transmission electron microscope

Usually, TEM is used to observe the morphology and dimension of the particles and macromolecules [43]. TEM images of HPS4-2A can be seen in Fig. A.2(c and d) of Appendix A. The observed polysaccharide exhibited spherical features arranged disorderedly. The diameters of the particle observed by TEM were in the range of 100–800 nm which weren't in agreement with that determined by MALLS. Apparently, the polysaccharide molecules were aggregated in water. There are two reasons for this phenomenon, one is the highly branched structure of HPS4-2A can entangled with each other in aqueous solution, which lead to aggregation, the other one is negative staining reagent changed the sample pH and ionic strength, which make aggregation is more obvious.

3.7.3. Atomic force microscope

The topographical AFM planar image of HPS4-2A deposited from a 1 μg/ml water solution was shown in Fig. 5. Pictures shown in Fig. 5 represent dilute regions within which individual molecules can be seen. Branched (arrows A), beadlike shape (arrows B), and irregular and spherical lumps (arrows C, arrows D) can be seen in Fig. 5a and b. The diameter and height of the lumps ranged from 10 to 100 nm and 5 to 50 nm, respectively. The heights of the spherical structures in Fig. 5c and d were much higher than that of a single polysaccharide chain (about 0.1–2 nm), suggesting that inter- and/or intra-molecular aggregation was involved. However, it was possible that the drying process could have some influence over the conformation of the molecules [44]. The results obtained in the present study were consistent with results obtained by SEM and SEC-MALLS.

The morphology observed under SEM has a clear distinction with the morphology observed by AFM. The reason was that the SEM used the lyophilized sample as observation object, and in freeze-drying process, water evaporating faster than natural-drying, therefore the polysaccharide molecules cannot stretched and stacked together to form a thin lamellar structure. While the atomic force microscope observation was carried out on the sample dried in the natural state, although the aggregation occurs in the drying process, still part of the polysaccharide molecules existed as stretched state.

3.8. Antioxidant activity

3.8.1. Effect of scavenging DPPH radicals

The ability of the HPS4-2A to scavenge DPPH radicals was shown in Fig. 6a and compared with that of ascorbic acid. DPPH radicals' scavenging rates of the HPS4-2A were dependent on its concentration; the scavenging rate at concentration of 8 mg/ml was 85.28% while the rate of ascorbic acid at the same

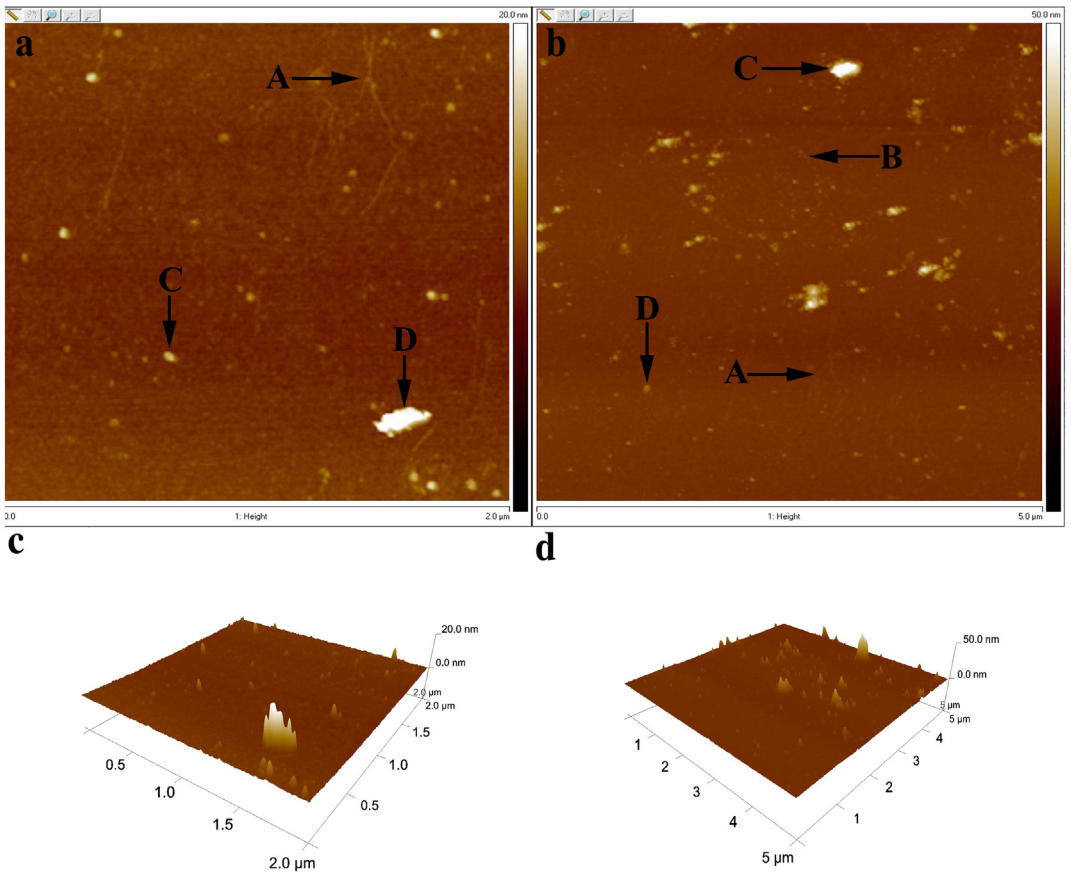

Fig. 5. Atomic force microscopy (AFM) planar (a and b) and cubic (c and d) images of HPS4-2A.

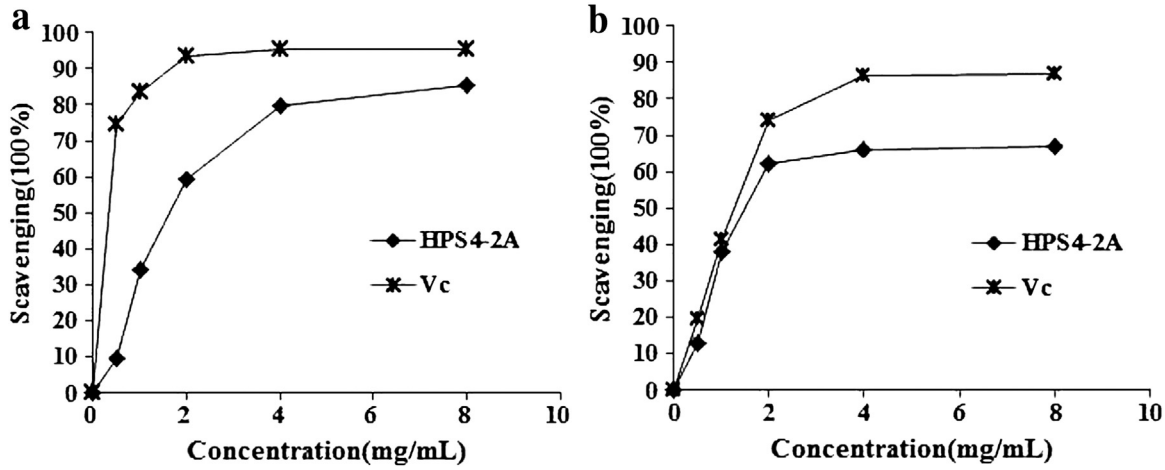

Fig. 6. Free-radical scavenging of HPS4-2A. DPPH radicals (a) and hydroxyl radicals (b).

concentration was 95.26%, suggesting good DPPH radicals' scavenging ability of HPS4-2A.

3.8.2. Measurement of hydroxyl radical scavenging activity

The result of hydroxyl free radical-scavenging ability of the HPS4-2A was shown in Fig. 6b and the ascorbic acid was regarded as positive control. The hydroxyl radical scavenging rate of HPS4-2A and ascorbic acid at 8.0 mg/ml was 66.93% and 87.01%, respectively, and in a concentration-dependent manner. This result proved that HPS4-2A had significant effect on scavenging hydroxyl radicals.

The antioxidant mechanism of Vitamin C and HPS4-2A is not identical. Vitamin C has antioxidant activity due to its enol group, which had strong reducing action. The antioxidant effect of HPS4-2A may be a result of combination of multiple mechanisms. According to the literatures [45–47], we can speculate the DPPH free radical scavenging mechanism of HPS4-2A may be due to its hydrogen-donating ability. DPPH radical was scavenged by HPS4-2A through donation of hydrogen to form a stable DPPH molecule [48]. Sulfate group act as an electrophile which promotes the intramolecular hydrogen donation [46,49–52], and resulting in enhancing DPPH radical scavenging capacity of HPS4-2A.

Both of the two mechanisms might be responsible for the hydroxyl radical scavenging ability of HPS4-2A as the earlier researchers suggested [52]: one suppresses the generation of the hydroxyl radical, and the other scavenges the hydroxyl radicals generated. HPS4-2A may ligate to the metal ions which react with hydrogen peroxide to give the metal complexes. The metal complexes thus formed could not further react with hydrogen peroxide to give hydroxyl radicals. As reported, in the absence of transition metal ions, hydrogen peroxide was fairly stable [53]. Radical scavenging ability of HPS4-2A was also related to the number of acetamido groups in a polysaccharide molecule, the existing of amino can enhance the radical scavenging ability, as Guo [54] reported. In addition, it has been reported that the antioxidant ability of the polysaccharide was bound up with monosaccharide composition [55] and molecular weight [56]. What described above was only a possible mechanism according to the speculation from the literatures, and the anti-oxidation mechanism of HPS4-2A is under in-depth studying now.

4. Conclusion

HPS4-2A, a heteropolysaccharide, which highly branched structure has been elucidated by SEC-MALLS, methylation analysis combined with GC–MS and 1D, 2D NMR spectroscopic technique. Its branched and spherical conformation has been studied by SEM, TEM and AFM. In summary, the backbone was composed of →4,6) α-D-Glcp (1→, →4,6) β-D-Galp (1→, →3,6) β-D-Galp (1→ and →3,4) 2-NAc-β-D-Galp (1→ (not common in plant polysaccharides) residues substituted at O-6, O-6, O-3 and O-4 positions, respectively. Side chains are terminated by arabinofuranosyl (Araf), glucopyranosyl (Glcp) residues and occasionally by SO_3^- (Shi also had similar findings in literature [7]. HPS4-2A exhibit strong antioxidant activities and further investigation on its antioxidant property in vivo and the others biological activities, especially radioprotective activity of HPS4-2A is in progress.

Acknowledgment

The authors would like to acknowledge the financial assistance provided by National "Twelfth Five-Year" Plan for Science & Technology Support (No. 2011BAI05B02) for supporting this research. The authors would like to thank Professor Wei Zhou, for providing instrumental facilities of GC–MS from Gansu entry–exit inspection and quarantine bureau. The authors would also like to express gratitude to College of chemistry and chemical engineering of Lanzhou University for the NMR spectra and elemental analysis. The authors would also like to express their appreciation to Lanzhou Institute of Chinese Physics, Chinese Academy of Sciences, for providing AFM, TEM, and SEM analyses.

Appendix A. Supplementary data

Supplementary data to this article can be found online at http://dx.doi.org/10.1016/j.fitote.2013.05.011.

References

[1] China Pharmacopoeia Committee. Pharmacopoeia of People's Republic of China. Beijing: Chemical Industry Press; 2010142.
[2] Kou JP, Zhu HR, Tang XJ, Tong CN. Effects of aqueous extract and ethanol extract from Radix Hedysari (RHA and RHE) on hemorrheology. Pharmacol Clin Chin Mater Med 2003;19:22–4.
[3] Li SG, Wang DG, Tian W, Wang XX, Zhao JX, Liu Z, et al. Characterization and anti-tumor activity of a polysaccharide from Hedysarum polybotrys Hand.-Mazz. Carbohydr Polym 2008;73:344–50.
[4] Zhao LG, Li XD, Zhao JH, Hu FD, Feng SL. The influence of four kinds of HPS to blood sugar of experimental diabetic mice. China Tradit Herb Drugs 2009;32:1590–2.
[5] Hui HP, Feng SL, Hu FD, Cui F, Wu YQ. Study on antioxidative activity of polysaccharide from radix hedysari in vitro. J Anhui Agric Sci 2010;38: 4056–7.
[6] Sun QX, Zheng YX, Su JP, Huang ZL. Anti-aging research of polysaccharide from Radix Hedysari. J Chin Med Mater 1994;11:42–3.
[7] Shi YK, Zhao LG, Liu XH, Hu FD, Cui F, Bi YY. Structural characterization of a sulfated glucan isolated from the aqueous extract of Hedysarum polybotrys Hand.-Mazz. Carbohydr Polym 2012;87:160–9.
[8] Lu MK, Cheng JJ, Lin CY, Chang CC. Purification, structural elucidation, and anti-inflammatory effect of a water-soluble 1, 6-branched 1, 3-α-D-galactan from cultured mycelia of Poria cocos. Food Chem 2010;118:349–56.
[9] Sun YL, Cui SW, Tang J, Gu XH. Structural features of pectic polysaccharide from *Angelica sinensis* (Oliv.) Diels. Carbohydr Polym 2010;80:544–50.
[10] Michel DB, Gilles KA, Hamilton JK, Rebers PA, Smith F. Colorimetric method for determination of sugars and related substances. Anal Chem 1956;28:350–6.
[11] Bradford MM. A rapid and sensitive method for the quantitation of microgram quantities of protein utilizing the principle of protein-dye binding. Anal Biochem 1976;72:248–54.
[12] Lehrfeld J. Simultaneous gas–liquid chromatographic determination of aldoses and alduronic acids. J Chromatogr 1987;408:245–53.
[13] Blumenkrantz N, Hansen GA. New method for quantitative determination of uronic acids. Anal Biochem 1973;54:484–9.
[14] Dang ZL, Liu XH, Zhao AN, Liang JD, Liang J, Feng SL. Chemical structural features and primary conformation of a neutral heteropolysaccharide HPS4-1A from *Hedysarum polybotrys* Hand.-Mazz. China Tradit Herb Drugs 2013;44:141–5.
[15] Sevage MG. Mechanism of the respiration of Pneumococci II. Anal Biochem 1934;273:419–29.
[16] Crowell EP, Burnett BB. Determination of the carbohydrate composition of wood pulps by gas chromatography of the alditol acetates. Anal Chem 1967;39:121–4.
[17] Needs PW, Selvendran RR. Avoiding oxidative degradation during sodium hydroxidemethyl iodide-mediated carbohydrate methylation in dimethyl sulfoxide. Carbohydr Res 1993;245:1–10.
[18] Harris PJ, Henry RJ, Blakeney AB, Stone BA. An improved procedure for the methylation analysis of oligosaccharides and polysaccharides. Carbohydr Res 1984;127:59–73.
[19] Foschiatti M, Hearshaw M, Paola C, Ravenscroft N, Rizzo R. Conformational studies of the capsular polysaccharide produced by *Neisseria meningitidis* group A. Carbohydr Res 2009;344:940–3.
[20] Yang HS, Lai SJ, An HJ, Li YF. Atomic force microscopy study of the ultrastructural changes of chelate-soluble pectin in peaches under controlled atmosphere storage. Postharvest Biol Technol 2006;39: 75–83.
[21] Shimada K, Fujikawa K, Yahara K, Nakamura T. Antioxidative properties of xanthone on the auto oxidation of soybean in cylcodextrin emulsion. J Agric Food Chem 1992;40:945–8.
[22] Chen Y, Xie MY, Nie SP, Li C, Wang YX. Purification, composition analysis and antioxidant activity of a polysaccharide from the fruiting bodies of *Ganoderma atrum*. Food Chem 2008;107:231–41.
[23] Wang JL, Zhang J, Wang XF, Zhao BT, Wu YQ, Yao J. A comparison study on microwave-assisted extraction of *Artemisia sphaerocephala* polysaccharides with conventional method: molecule structure and antioxidant activities evaluation. Int J Biol Macromol 2009;45:483–92.
[24] Zhang LS, Wang X, Dong LL. Antioxidation and antiglycation of polysaccharides from *Misgurnus anguillicaudatus*. Food Chem 2011;124: 183–7.
[25] Podzimek S. Light scattering, size exclusion chromatography and asymmetric flow field flow fractionation.New Jersey: John Wiley & sons, Inc., Hoboken Publisher; 2011IX [100, 207].
[26] Carpita NC, Shea EM. Linkage structure of carbohydrate by gas chromatography–mass spectrometry (GC–MS) of partially methylated alditol acetates. In: Biermann CJ, McGinnis GD, editors. Analysis of carbohydrates by gas–liquid chromatography and mass spectrometry. Florida: CRC Press; 1989. p. 157–216.
[27] Cui WW, Eskin MN, Biliaderis CG, Marat K. NMR characterization of a 4-O-methyl-β-D-glucuronic acid-containing rhamnogalacturonan from yellow mustard (*Sinapis alba* L.) mucilage. Carbohydr Res 1996;292: 173–83.
[28] Jahanbin K, Gohari AR, Moini S, Djomeh ZE, Masi P. Isolation, structural characterization and antioxidant activity of a new water-soluble polysaccharide from *Acanthophyllum bracteatum* roots. Int J Biol Macromol 2011;49:567–72.
[29] Roy SK, Das D, Mondal S, Maiti D, Bhuni B, Maiti TK, et al. Structural studies of an immunoenhancing water-soluble glucan isolated from hot water extract of an edible mushroom, *Pleurotus florida*, cultivar Assam Florida. Carbohydr Res 2009;344:2596–601.
[30] Niu YG, Wang HY, Xie ZH, Whent M, Gao XD, Zhang X, et al. Structural analysis and bioactivity of a polysaccharide from the roots of *Astragalus membranaceus* (Fisch) Bge. var. mongolicus (Bge.) Hsiao. Food Chem 2011;128:620–6.
[31] Cao W, Li XQ, Liu L, Yang TH, Li C, Fan HT, et al. Structure of an anti-tumor polysaccharide from *Angelica sinensis* (Oliv.) Diels. Carbohydr Polym 2006;66:149–59.
[32] Wu YL, Sun CR, Pan YJ. Studies on isolation and structural features of a polysaccharide from the mycelium of an Chinese edible fungus (*Cordyceps sinensis*). Carbohydr Polym 2006;63:251–6.
[33] Liu CH, Lin QX, Gao Y, Ye L, Xing YY, Xi T. Characterization and antitumor activity of a polysaccharide from Strongylocentrotus nudus eggs. Carbohydr Polym 2007;67:313–8.
[34] Senchenkova SN, Perepelov AV, Cedzynski M, Swierzko AS, Ziolkowski A, Shashkov AS, et al. Structure of a highly phosphorylated O-polysaccharide of *Proteus mirabilis* O41. Carbohydr Res 2004;339:1347–52.
[35] Parkhomchuk AA, Kocharova NA, Kokot MB, Shashkov AS. Structure of the O-polysaccharide from the lipopolysaccharide of *Providencia alcalifaciens* O12. Carbohydr Res 2010;345:1235–9.
[36] Moreau M, Richards JC, Perry MB. Application of high-resolution N.M.R. spectroscopy to the elucidation of the structure of the specific capsular polysaccharide of *Streptococcus pneumoniae* type 7F. Carbohydr Res 1988;182:79–99.
[37] Kang J, Cui SW, Phillips GO, Chen J, Guo QB, Wang Q. New studies on gum ghatti (*Anogeissus latifolia*) Part III: Structure characterization of a globular polysaccharide fraction by 1D, 2D NMR spectroscopy and methylation analysis. Food hydrocoll 2011;25:1999–2007.
[38] Das D, Mondal S, Roy SK, Maiti D, Bhunia B, Maiti TK, et al. Isolation and characterization of a heteropolysaccharide from the corm of *Amorphophallus campanulatus*. Carbohydr Res 2009;344:2581–5.
[39] Ponder GR, Richards GN. Arabinogalactan from Western Larch, part II; a reversible order-disorder transition. J Carbohydr Chem 1997;16:195–211.
[40] Laws AP, Chadha MJ, Romero MC, Marshall VM, Maqsood M. Determination of the structure and molecular weights of the exopolysaccharide produced by *Lactobacillus acidophilus* 5e2 when grown on different carbon feeds. Carbohydr Res 2008;343:301–7.
[41] Cimino P, Bifulco G, Casapullo A, Bruno I, Paloma LG, Riccio R. Isolation and NMR characterization of rosacelose, a novel sulfated polysaccharide from the sponge *Mixylla rosacea*. Carbohydr Res 2001;334:39–47.
[42] Robic A, Gaillard C, Sassi JF, Lerat Y, Lahaye M. Ultrastructure of ulvan: a polysaccharide from green seaweeds. Biopolymers 2009;91:655.
[43] Yong ZT, Zhang LN. Determination of molecular size and shape of hyperbranched polysaccharide in solution. Biopolymers 2006;83: 414–23.
[44] Kirby AR, Gunning AP, Morris VJ. Imaging xanthan gum by atomic force microscopy. Carbohydr Res 1995;267:161–6.
[45] Chen HX, Zhang M, Xie BJ. Components and antioxidant activity of polysaccharide conjugate from green tea. Food Chem 2005;90:17–21.
[46] Tsiapali E, Whaley S, Kalbfleisch J, Ensley HE, Browder IW, Williams DL. Glucans exhibit weak antioxidant activity, but stimulate macrophage free radical activity. Free Radic Biol Med 2001;30:393–402.
[47] Song HF, Zhang QB, Zhang ZS, Wang J. In vitro antioxidant activity of polysaccharides extracted from *Bryopsis plumose*. Carbohydr Polym 2010;80:1057–61.
[48] Matthaus B. Antioxidant activity of extracts obtained from residues of different oilseeds. J Agric Food Chem 2002;50:3444–52.
[49] Qi HM, Zhang QB, Zhao TT, Chen R, Zhang H, Niu XZ, et al. Antioxidant activity of different sulfate content derivatives of polysaccharide extracted from *Ulva pertusa* (Chlorophyta) in vitro. Int J Biol Macromol 2005;37:195–9.

[50] Xing RE, Liu S, Guo ZY, Yu HH, Wang PB, Li CP. Relevance of molecular weight of chitosan and its derivatives and their antioxidant activities in vitro. Bioorg Med Chem 2005;13:1573–7.
[51] Zhu BW, Zhou DY, Li T, Yan S, Yang JF, Li DM, et al. Chemical composition and free radical scavenging activities of a sulphated polysaccharide extracted from abalone gonad (Haliotis Discus Hannai Ino). Food Chem 2010;121:712–8.
[52] Ueda J-i, Saito N, Shimazu Y, Ozawa T. A comparison of scavenging abilities of antioxidants against hydroxyl radicals. Arch Biochem Biophys 1996;333:377–84.
[53] Wang J, Zhang QB, Zhang ZS, Li ZE. Antioxidant activity of sulfated polysaccharide fractions extracted from *Laminaria japonica*. Int J Biol Macromol 2008;42:127–32.
[54] Guo ZY, Xing RE, Liu S, Yu HH, Wang PB, Li CP, et al. The synthesis and antioxidant activity of the Schiff bases of chitosan and carboxymethyl chitosan. Bioorg Med Chem Lett 2005;15:4600–3.
[55] Bi HT, Gao TT, Li ZH, Ji L, Yang W, Jeff Iteku B, et al. Structural elucidation and antioxidant activity of a water-soluble polysaccharide from the fruit bodies of *Bulgaria inquinans* (Fries). Food Chem 2013;138:1470–5.
[56] Liu DM, Sheng JW, Li ZJ, Qi HM, Sun YL, Duan Y, et al. Antioxidant activity of polysaccharide fractions extracted from *Athyrium multidentatum* (Doll.) Ching. Int J Biol Macromol 2013;56:1–5.